The Journal of Infectious Diseases

MAJOR ARTICLE

Clonal Hematopoiesis Is Associated With Low CD4 Nadir and Increased Residual HIV Transcriptional Activity in Virally Suppressed Individuals With HIV

Wouter A. van der Heijden,[1,2,a] Rosanne C. van Deuren,[1,3,4,a] Lisa van de Wijer,[1,2] Inge C. L. van den Munckhof,[1,3] Marloes Steehouwer,[3,4] Niels P. Riksen,[1,3] Mihai G. Netea,[1,3,5] Quirijn de Mast,[1,2] Linos Vandekerckhove,[6] Richarda M. de Voer,[3,4] Andre J. van der Ven,[1,2] and Alexander Hoischen[1,3,4]

[1]Department of Internal Medicine, Radboud Center for Infectious Diseases, Radboud University Medical Center, Nijmegen, the Netherlands, [2]Radboud Institute for Health Sciences, Radboud University Medical Center, Nijmegen, the Netherlands, [3]Radboud Institute for Molecular Life Sciences, Radboud University Medical Center, Nijmegen, the Netherlands, [4]Department of Human Genetics, Radboud University Medical Center, Nijmegen, the Netherlands, [5]Department for Genomics and Immunoregulation, Life and Medical Sciences Institute, University of Bonn, Bonn, Germany, and [6]HIV Cure Research Center, Department of Internal Medicine and Pediatrics, Faculty of Medicine and Health Sciences, Ghent University and Ghent University Hospital, Ghent, Belgium

Clonal hematopoiesis, a common age-related phenomenon marked by expansion of cells with clonal hematopoiesis driver mutations, has been associated with all-cause mortality, cancer, and cardiovascular disease. People with HIV (PWH) are at risk for non-AIDS–related comorbidities such as atherosclerotic cardiovascular disease and cancer. In a cross-sectional cohort study, we compared clonal hematopoiesis prevalence in PWH on stable antiretroviral therapy with prevalence in a cohort of overweight individuals and a cohort of age- and sex-matched population controls. The prevalence of clonal hematopoiesis adjusted for age was increased and clone size was larger in PWH compared to population controls. Clonal hematopoiesis is associated with low CD4 nadir, increased residual HIV-1 transcriptional activity, and coagulation factors in PWH. Future studies on the effect of clonal hematopoiesis on the HIV reservoir and non-AIDS–related comorbidities are warranted.

Keywords. HIV; clonal hematopoiesis; cART toxicity; coagulation; inflammation.

People with human immunodeficiency virus (PWH) are at risk for non-AIDS–related comorbidities such as atherosclerotic cardiovascular disease (CVD) and cancer [1, 2]. This risk is associated with persistent inflammation, increased coagulation, accelerated aging, CD4 nadir, and certain antiretroviral drugs [1].

Recently, clonal hematopoiesis (CH), a common age-related phenomenon marked by expansion of cells with CH driver mutations, has been associated with all-cause mortality, cancer, and CVD [3–5]. Aside from age, chronic infection [6] and inflammation [7, 8] have also been implicated in the development of CH. As PWH experience persistent inflammation and are at increased risk for accelerated aging and CVD [9, 10], a role for CH in PWH is therefore hypothesized. Indeed, a recent study observed increased prevalence of CH as detected by whole-exome sequencing (WES) in PWH as compared to controls [11]. However, associations with human immunodeficiency virus (HIV)-related factors and risk factors of CVD and cancer in PWH, such as the viral reservoir, CD4 nadir, or inflammation, were not shown. As the clinical course and treatment of HIV infection and CH possibly converge on hematopoietic stem cell biology, a potential correlation deserves investigation. Additionally, like many other large-scale CH studies, the study [11] used WES and as such could only detect mutations of considerable size (≥2%, also called CH of indeterminate potential [CHIP] mutations), whereas the use of targeted sequencing techniques improves the sensitivity for the detection of smaller CH driver mutations [12]. The aim of our study was to determine CH prevalence in PWH as compared to controls, and to assess possible associations with HIV-related clinical parameters and markers of HIV reservoir, coagulation, and inflammation.

METHODS

Study Subjects

Samples were obtained from the 200HIV cohort (PWH cases, n = 219) [13] on combination antiretroviral therapy (cART) with plasma HIV RNA <200 copies/mL, 300-Obese cohort (HIV-uninfected, overweight controls, body mass index [BMI] > 27 kg/m^2, n = 302) [14], and Nijmegen Biomedical Study (NBS; HIV-uninfected population controls, n = 437) [15]. The 200HIV

Received 8 February 2021; editorial decision 16 August 2021; accepted 18 August 2021; published online August 21, 2021.

[a]W. A. H. and R. C. D. contributed equally.

Correspondence: Wouter A. van der Heijden, MD, Department of Internal Medicine, Radboud University Medical Center, PO Box 9101, 6500 HB Nijmegen, the Netherlands (Wouter.vanderheijden@radboudumc.nl).

The Journal of Infectious Diseases® 2022;225:1339–47

https://doi.org/10.1093/infdis/jiab419

and 300-Obese cohort are both part of the Human Functional Genomics Project (www.humanfunctionalgenomicsproject.org) enrolled at the Radboud University Medical Center, Nijmegen, the Netherlands. These studies were approved by the local ethics committee (CMO Arnhem-Nijmegen, 200HIV: NL3235709110; 300-Obese: NL4684609113) and conducted in accordance with the Declarations of Helsinki. Samples for DNA extraction and plasma measurement were obtained after written informed consent. Clinical data were extracted from the electronic medical records and/or from the Dutch HIV registry (Stichting HIV-monitoring). The NBS is a population-based study of 9350 individuals, based on age- and sex-stratified random sample from the register of municipality of Nijmegen, the Netherlands [15].

Clonal Hematopoiesis Mutation Identification

CH mutations were analyzed in DNA isolated from whole blood in PWH and 300-Obese cohorts, using ultrasensitive single-molecule molecular inversion probe (smMIP) sequencing, as previously described [16]. In short, a total of 300 MIP probes were designed covering CH-related hotspots in 24 genes, including *ASXL1*, *TET2*, and *DNMT3A* (Supplementary Table 1 and Supplementary Table 2). In addition, we selected 437 age- and sex-matched population control samples, and used the previously generated sequencing data for CH mutation identification, but due to subtle technical (probe density) differences excluded *DNMT3A* mutations from this direct comparison [15]. For each individual, 2 technical (polymerase chain reaction [PCR]) replicates were sequenced, after which 2 independent data processing strategies were applied followed up by a targeted quality control (Supplementary Figure 1). Raw sequencing data were converted to fastQ files, which were (1) aligned to the reference genome (hg19) using Burrows-Wheeler Aligner with Maximal Exact Match (BWA-MEM) [17] and (2) imported into the commercially available next-generation sequencing software package Sequence Pilot (JSI Medical Systems), using the optimized smMIP analysis module as described previously [18, 19]. The latter allows for a consensus calling per probe, enabling somatic calls down to 0.001% (depending on locus specific coverage) by using a majority vote of unique molecular identifier duplicates. The resulting variant calls were then subjected to a stringent quality filtering pipeline (Supplementary Figure 1C), in which (likely) false-positive calls were excluded. The final variant allele frequency was calculated using samtools mpileup [20] on the aligned bamfiles from (1). PWH and 300-Obese samples with an average coverage over the entire panel, and population control samples over all non-*DNMT3A* genes, of >500× were included for analysis. We classified all detected CH mutations in 2 categories: (1) large clones, CH mutations with a variant allele frequency ≥2%, an arbitrary threshold established in the current literature historically chosen for methodological reasons [21]; and (2) small clones, CH mutations with a variant allele frequency <2%.

Circulating Factors

Circulating factors of inflammation interleukin 18 (IL-18), high-sensitivity C-reactive protein (hsCRP), sCD14, and sCD163 were measured using enzyme-linked immunosorbent assay (ELISA; Duoset or Quantikine, R&D Systems). D-dimer was measured by ELISA according manufacturer's instructions (Abcam). IL-6, tumor necrosis factor-α (TNF-α), IL-10, and IL-1Ra in serum were measured using Simple Plex Cartridges (Protein Simple, R&D Systems). All assays were performed according to manufacturer's recommendations. Von Willebrand factor (vWF) concentrations were performed with an in-house sandwich ELISA assay (DAKO, Agilent) [22].

HIV-1 Reservoir Quantification

HIV-1 Cell-associated HIV-1 DNA (CA-DNA) and Cell-associated HIV-1 RNA (CA-RNA) in $CD4^+$ cells were isolated using EasySep Human $CD4^+$ T Cell Isolation Kit (Stemcell Technologies) and were measured in triplicate by droplet digital PCR (ddPCR; QX200, Bio-Rad) as described previously [23]. Genomic DNA was extracted using the DNeasy Blood and Tissue kit (Qiagen) according to the manufacturer's protocol with an additional step of adding 75 µL elution buffer on the column heated at 56°C for 10 minutes. CA-RNA was extracted using the Innuprep RNA kit (Westburg). RNA was reversely transcribed to cDNA by qScript cDNA SuperMix (Quantabio). Before PCR amplification, genomic DNA was restricted by EcoRI (Promega) [23]. Total HIV-1 DNA measurements were normalized by measuring the reference gene *RPP30* in duplicate by ddPCR and expressed per million $CD4^+$ cells. CA-RNA was normalized using 3 reference genes, (*B2M*, *ACTB*, and *GADPH*) determined by LightCycler 480 SYBR Green I Master mix. HIV-1 RNA copies were divided by the geometric mean of the reference genes and expressed per million $CD4^+$ cells. Droplet classification and absolute quantification were performed using the ddpcRquant analysis tool with standard settings [24]. Primers and probes are shown in Supplementary Table 3.

Statistical Analysis

All analyses were performed in R version 3.6.1 (R Core Team, CRAN-project). *P* values < .05 were considered statistically significant. General characteristics were compared by means of Wilcoxon-rank sum tests for continuous parameters and χ^2 tests for categorical parameters. In addition, we computed standardized mean differences where appropriate using the R package stddiff.

CH mutation prevalence in PWH versus 300-Obese was assessed first by means of χ^2 tests and second in a logistic regression model correcting for the known risk factor age and cohort (a variable indicating whether an individual is in the PWH or 300-Obese). Prevalence of non-*DNMT3A* CH mutations in PWH versus population controls was assessed in

the same way. Logistic model fit was evaluated by means of a givitiCalibrationBelt plot using the package givitiR, and are shown in Supplementary Figure 2.

To assess whether different mutational processes contribute to CH mutations in PWH as compared to controls, we performed a mutational signature analysis studying all 48 single base substitutions (SBS) in their 3-nucleotide context (Supplementary Table 4) [25]. Fitting all identified somatic mutations into existing SBS signatures for which mutational processes of both endogenous and exogenous origin have been characterized, may allow the identification of differential mutation processes for different sets of mutations. The contribution of the SBS signatures was inferred using the R package DeconstructSigs [26] and Mutational Signatures version 3.1 available at the Catalogue of Somatic Mutations in Cancer (COSMIC release version 91, June 2020).

Within PWH differences in categorical parameters were assessed by means of χ^2 tests, and continuous parameters by means of Wilcoxon-rank sum tests. In addition, to explore possible factors that are correlated with CH in PWH, we performed stepwise logistic regression with a selection of clinically relevant parameters as independent variables, CH mutation prevalence as dependent variable using the stepAIC() function with direction = "both" from the MASS package.

All figures were likewise generated in R using a variety of packages (dplyr, reshape2, ggplot2, ggpubr, tidyverse, ggpmisc, rcompanion, ggbeeswarm), after which they were optimized in Adobe Illustrator version 23.1.1.

RESULTS

A total of 217 PWH on cART, 297 uninfected 300-Obese control, and 399 age- and sex-matched population control individuals passed our quality control and coverage threshold of 500× (Supplementary Figure 3), and were included in our analyses. The age of PWH individuals ranged from 24 to 74 years, with an average age of 51.3 years, and the majority were male (n = 199, 91.7%). HIV-uninfected overweight controls (300-Obese) were generally older (age range 54–81 years, average age 67.1 years), and sex was more evenly distributed (male n = 134, 45.1%). The age and sex distribution of our included population controls was comparable to PWH individuals, with an age ranging from 24 to 69 years and an average of 51.9 years, and the majority of individuals were male (n = 365, 91.5%).

CH Mutation Prevalence in PWH Versus Uninfected Controls

We identified 51 candidate CH mutations in 46 PWH individuals (21.2%), 5 individuals presenting with 2 different mutations. General characteristics for PWH CH mutation carriers versus noncarriers are shown in Table 1. The variant allele frequency of all CH mutations ranged from 0.05% to 32.94%, with a median clone size of 1.01%. Out of 51 mutations, 20 (39.2%) were categorized as large clones (≥2%), highlighting the sensitivity of our assay to detect somatic mutations below the arbitrary allele frequency cutoff for CHIP [3, 15]. For a complete list of all identified candidate CH mutations see Supplementary Table 5.

In our HIV-uninfected overweight controls (300-Obese), we identified 110 candidate CH mutations in 85 individuals (28.6%). We were unable to detect a significant difference in either CH mutations or CHIP prevalence between PWH and overweight controls (Supplementary Table 6). However, after correcting for the most important known risk factor, age, in a logistic model, we identified that the probability of CHIP in PWH is significantly higher as compared to HIV-uninfected overweight controls (odds ratio [OR], 2.211; 95% confidence interval [CI], 1.025-4.769), an effect that did not reach statistical significance when smaller clones (variant allele frequency <2%) were included (Supplementary Table 7). Most observed clones in PWH were mutations in *DNMT3A*, representing roughly half of the CH mutations per age category (Figure 1A). Comparing the gene occurrence in PWH aged ≥55 years to controls aged ≥55 years, we observed that the proportion of CH mutations in genes other than *DNMT3A*, specifically *JAK2, STAT3*, and *TP53*, was larger in PWH (Figure 1B), whereas on average CH mutation size was not different (Figure 1C). Considering only non-*DNMT3A* mutations in our age- and sex-matched population controls, we identified 55 candidate CH mutations in 42 individuals (10.5%), as compared to 25 in 23 individuals (10.6%) in PWH. Even though there was no significant difference in raw prevalence ($P = 1.00$), logistic regression revealed that the effect of age on CH mutation prevalence was significantly smaller in PWH as compared to population controls, suggesting that non-age–related factor(s) drive(s) the prevalence of CH in PWH (Supplementary Table 7). Finally, non-*DNMT3A* CH mutations were significantly larger in size in PWH as compared to population controls ($P = .004$; Figure 1D).

CH Mutations in PWH Individuals Are Possibly Driven by Different Mutational Processes

To understand the mutational processes contributing to CH mutations, we explored mutational signatures, that is base substitutions in a trinucleotide context [25]. Our mutational signature analysis identified that the signatures SBS1 (clock-like signature) and SBS18 (reactive oxygen species [ROS] signature) contributed uniquely to CH mutations in PWH, whereas SBS6 and SBS21 (both involved in DNA mismatch repair) contributed uniquely to CH mutations in HIV-uninfected overweight controls (Figure 2A). Remarkably, SBS18, a signature predominantly characterized by C>A mutations, was likewise identified as contributing to CH mutations in PWH with prior exposure to zidovudine (AZT), whereas it was absent in unexposed individuals (red dashed box in Figure 2A and 2B). However, as the number of CH mutations in this last subgroup analysis is low,

Table 1. General Characteristics of PWH Without CH Mutations (Noncarriers) Compared to PWH With 1 or More Identified CH Mutations (CH Carriers)

Characteristic	Noncarriers (n = 171)	CH Carriers (n = 46)	P Value
Sex, female, n (%)	13 (7.6)	5 (10.9)	.68
Age, y, mean (IQR)	50.0 (44.0–58.0)	57.0 (48.0–62.2)	**.006**
BMI, kg/m^2, mean (IQR)	24.2 (22.0–26.5)	23.7 (22.4–25.8)	.48
Known duration of HIV infection, y, mean (IQR)	7.5 (4.7–12.7)	10.6 (6.8–16.9)	**.03**
Way of transmission, n (%)			.44
Heterosexual	8 (4.7)	1 (2.2)	
IDU	2 (1.2)	1 (2.2)	
MSM	132 (77.2)	32 (69.6)	
Other/unknown	29 (17.0)	12 (26.1)	
CD4 nadir, cells/µL, mean (IQR)	270.0 (150.0–380.0)	195.0 (72.5–290.0)	**.001**
Current CD4 T-cell count, cells/µL, mean (IQR)	660.0 (490.0–805.0)	635.0 (472.5–755.0)	.58
Current CD4/CD8 T-cell ratio, mean (IQR)	0.8 (0.6–1.1)	0.8 (0.6–1.2)	.37
Zenith HIV RNA, copies/mL, median (IQR)	100 000.0 (60 000.0–400 000.0)	70 000.0 (30 281.5–222 250.0)	**.04**
HIV RNA >50 copies/mL <1 y prior to inclusion, n (%)	14 (8.2)	9 (19.6)	.052
cART duration, y, mean (IQR)	6.1 (3.7–10.2)	9.1 (4.4–16.8)	.05
ARV class, n (%)			
NRTI	165 (96.5)	44 (95.7)	1
NtRTI	79 (46.2)	23 (50.0)	.77
NNRTI	50 (29.2)	13 (28.3)	1
PI	21 (12.3)	11 (23.9)	.08
AZT ever, n (%)	39 (23.2)	18 (39.1)	**.048**
Cardiovascular risk factors, no, n (%)	45 (26.3)	6 (13.0)	.09
Prior MI/CVA, yes, n (%)	11 (6.4)	5 (10.9)	.48
Active smoking, n (%)	44 (25.7)	17 (37.0)	.19
Pack years, mean (IQR)	12.0 (0.0–27.0)	18.5 (1.9–35.1)	.18
Hypercholesterolemia, n (%)	45 (26.3)	13 (28.3)	.94
Hypertension, n (%)	33 (19.3)	10 (21.7)	.87
Diabetes mellitus, n (%)	9 (5.3)	1 (2.2)	.62
Family history CVD, 1st-degree relative, n (%)	81 (47.4)	26 (56.5)	.35

Wilcoxon-rank sum test or χ^2 test *P* value are given where applicable. Bold font indicates significant P values (<.05).

Abbreviations: ARV, antiretroviral drug; AZT, zidovudine; BMI, body mass index; cART, combination antiretroviral therapy; CH, clonal hematopoiesis; CVA, cerebrovascular accident; CVD, cardiovascular disease; HIV, human immunodeficiency virus; IDU, intravenous drug use; IQR, interquartile range; MI, myocardial infarction; MSM, men who have sex with men; NNRTI, nonnucleoside reverse transcriptase inhibitor; NRTI, nucleoside reverse transcriptase inhibitor; NtRTI, nucleotide reverse transcriptase inhibitor; PI, protease inhibitor; INSTI, integrase inhibitor; PWH, people with HIV.

the corresponding cosine value indicates these results should be interpreted with caution.

Low CD4 Nadir, Markers of Coagulation, and HIV Reservoir Are Associated With CH Mutation Prevalence in PWH

Subsequently, we explored the clinical correlates of PWH with their CH mutation carrier status. In these exploratory analyses, CH mutation carriers were older (*P* = .006; Table 1), duration of known HIV infection was longer (*P* = .026; Table 1), and CD4 nadir was lower (*P* = .001; Figure 3A). There was no difference in CH mutation prevalence with regard to cART regimens, CD4/CD8 T-cell ratio, or current CD4 T-cell count. In a logistic regression model, older age (OR [+5 years], 1.205; 95% CI, 1.013–1.450; *P* = .04), lower CD4 nadir (OR [+50 cells/mm^2], 0.794; 95% CI, .687–.907; *P* = .001), increased CD4/CD8 ratio (OR, 2.850; 95% CI, 1.334–6.391; *P* = .008) were independently correlated with CH mutation prevalence, whereas HIV duration and current CD4 T-cell count were not (Supplementary Table 7).

PWH with a CH mutation were more likely to have had at least once a viral load of >50 copies/mL 1 year prior to study visit (19.6% vs 8.2%, *P* = .052), suggesting a more active HIV reservoir. In virally suppressed PWH, the HIV-1 CA-DNA roughly equals total integrated proviral DNA, while HIV-1 CA-RNA is associated with HIV-1 transcriptional activity [27]. Although these parameters of HIV reservoir strongly intercorrelate, HIV CA-RNA was increased in CH mutation carriers and HIV CA-DNA was not (Figure 3B). The discrepancy between CA-RNA and CA-DNA suggests an effect on transcriptional activity [27]. As a result, PWH with viral load between 50 and 200 copies/mL (viral blip) 1 year prior to study visit (10.6%) had higher levels of CA-RNA (*P* < .01) but no differences in CA-DNA. Although the CA-RNA difference disappeared after correction for CD4 nadir and age (Supplemental Table 7), the ratio of HIV-1 CA-RNA to CA-DNA, which represent relative viral transcription level [27], was increased in CH mutation carriers (OR, 5.563; 95% CI, 1.768–45.970; *P* = .017; Supplementary Table 7), independent of CD4 nadir, age, and CD4/CD8 T-cell ratio.

Additionally, we studied associations between CH mutation carriership, coagulation, and inflammation. No correlation was

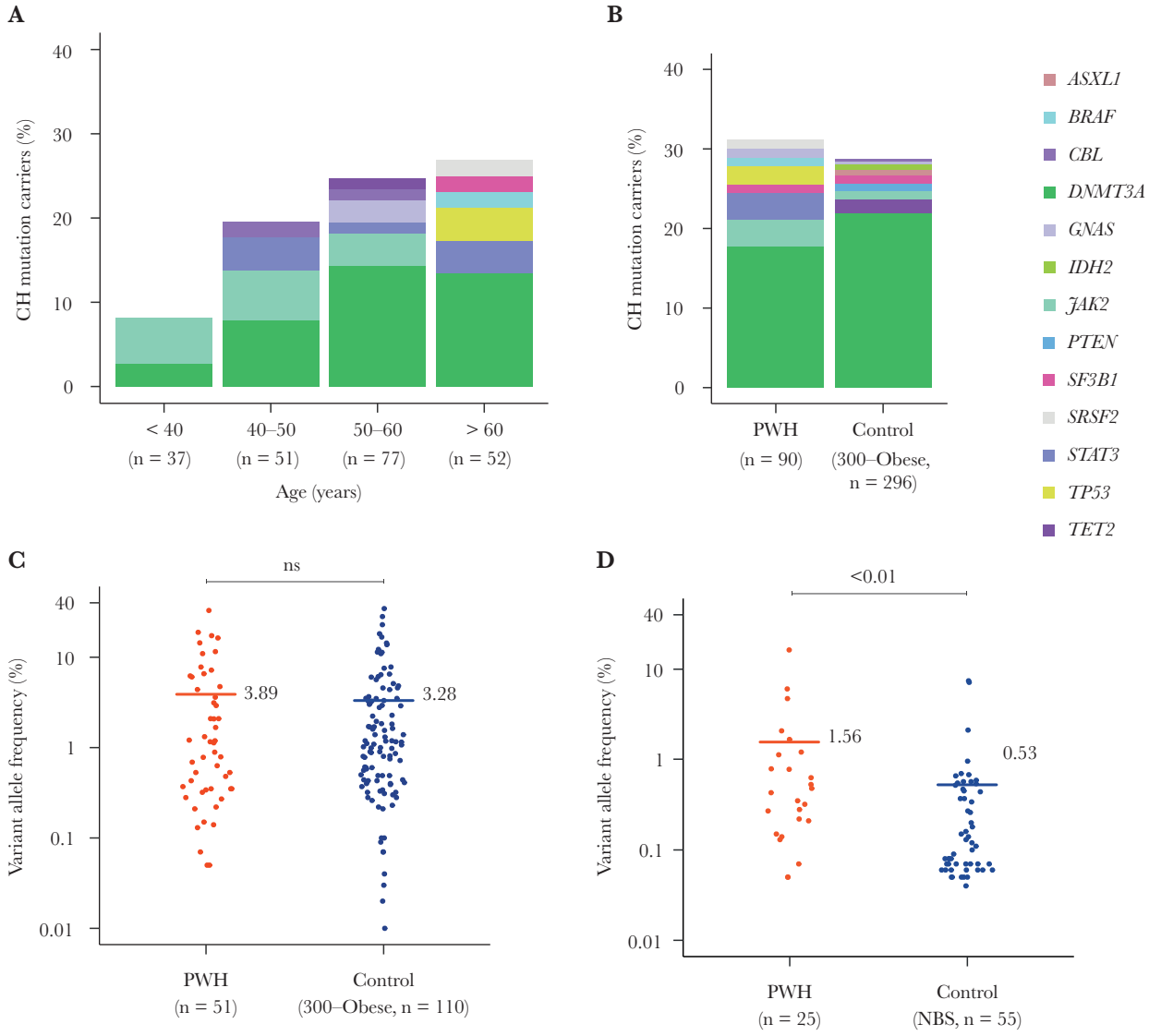

Figure 1. Clonal hematopoiesis (CH) mutations in people with HIV (PWH), HIV-uninfected overweight controls (300-Obese), and HIV-uninfected age- and sex-matched population controls (NBS). *A*, CH mutation prevalence increased with age in PWH. The stacked bars represent the percentage of PWH carrying a CH mutation per age category (the CH mutation with highest variant allele frequency is plotted for individuals carrying multiple mutations). *B*, The proportion of CH mutations in genes other than *DNMT3A* in PWH aged ≥55 years (n = 90) was larger compared to HIV-uninfected overweight controls (n = 296). *C*, CH mutation size nonsignificantly increased in PWH as compared to HIV-uninfected overweight controls. *D*, CH mutation size was significantly larger in PWH as compared to population controls. *C* and *D*, Each dot represents a CH mutation (the number of mutations is annotated on the x-axis and the size on the y-axis), with a horizontal line and number to the right indicating the mean CH mutation size and the Wilcoxon-rank sum test *P* value at the top.

found with circulating inflammation markers (hsCRP, sCD14, sCD163, IL-6), while coagulation markers (D-dimer and vWF) were increased in CH mutation carriers (Figure 3C and 3D and Supplementary Figure 4), independent of age, CD4 nadir, and CD4/CD8 T-cell ratio (vWF OR [+5000 ng/mL], 1.053; 95% CI, 1.014–1.097; $P = .009$; D-dimer OR [+50 mg/mL], 1.076; 95% CI, 1.004–1.163; $P = .044$; Supplementary Table 7).

DISCUSSION

In the current study, we show that CH driver mutations in PWH on long-term successful cART are common and are independently associated with older age, low CD4 nadir, and increased CD4/CD8 T-cell ratio, as well as with markers of coagulation. Furthermore, we show that CH is linked to increased relative HIV-1 transcription level (ie, increased HIV-1 CA-RNA to HIV-1 CA-DNA ratio).

Age is a known CH predictor in the general population [3, 4, 16], and an association was present in the current study, supporting the validity of our data. CH may be important in PWH as their presence has been associated with hematological (pre)malignancies, as well as with CVD and all-cause mortality in HIV-uninfected individuals [3]. Recently, a large-scale

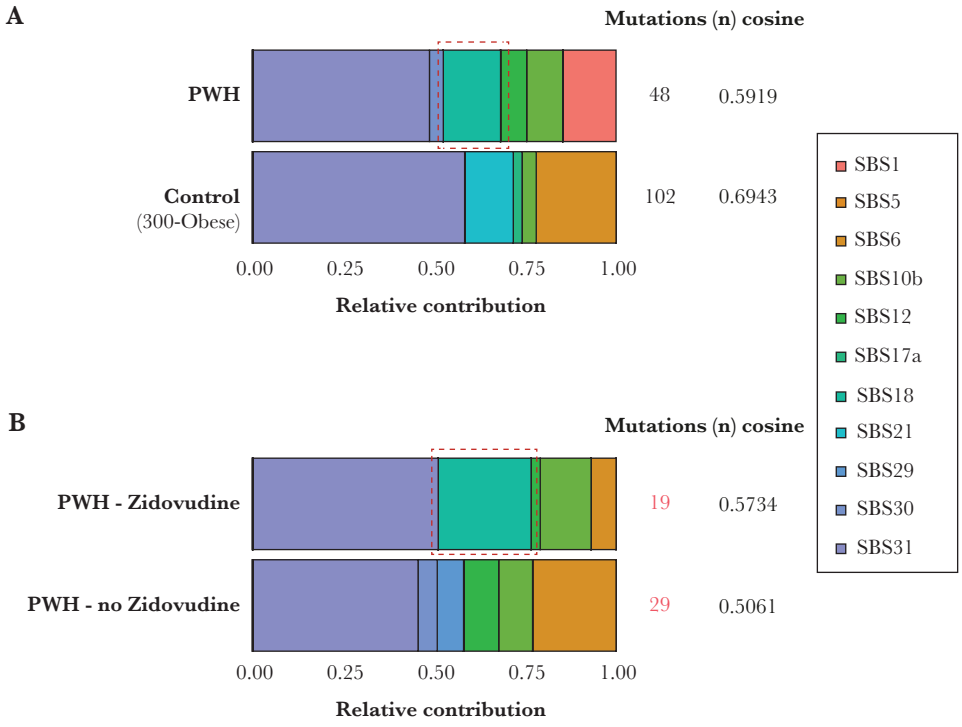

Figure 2. PWH present with a distinct mutational signature profile. *A*, Contribution of different SBS signatures to CH mutations in PWH (top) and HIV-uninfected overweight controls (bottom). SBS1 and SBS18 contributed uniquely to CH mutations in PWH, whereas SBS6 and SBS21 were unique to controls. For raw results see Supplementary Table 8A. *B*, SBS18 (red dashed box), a signature predominantly characterized by C>A mutations that is involved in ROS production, uniquely contributed to CH mutations in PWH with prior exposure to AZTs. For raw results see Supplementary Table 8B. Proposed etiology of SBS signatures: SBS1, spontaneous deamination of 5-methylcytosine (clock-like signature); SBS5, unknown (clock-like signature); SBS6, defective DNA mismatch repair; SBS10b, polymerase epsilon exonuclease domain mutations; SBS12, unknown; SBS17a, unknown; SBS18, damage by reactive oxygen species; SBS21, defective DNA mismatch repair; SBS29, tobacco chewing; SBS30, defective DNA base excision repair due to *NTHL1* mutations; SBS31, platinum chemotherapy treatment. Mutations (n) shows the number of CH mutations analyzed in each group; cosine represents the cosine similarity value (range 0–1), a correction applied on mutations prior to fitting to SBS signatures, values <0.8 are considered low. Abbreviations: AZT, zidovudine; CH, clonal hematopoiesis; HIV, human immunodeficiency virus; PWH, people with HIV; ROS, reactive oxygen species; SBS, single base substitution.

CH study by Bick et al reported increased prevalence of large clones, or CHIP, in PWH as compared to control individuals [11]. In line with this, the probability of large clones, adjusted for age, was increased in PWH as compared to HIV-uninfected overweight controls, and the probability of all non-*DNMT3A* clones (small and large) was intriguingly driven by something other than age in PWH as compared to population controls in the present study. Consistent with the latter, and the hypothesis that time is needed for a clone to grow, clone size was significantly increased in PWH as compared to age- and sex-matched population controls. The absence of this in our PWH versus overweight controls comparison is most likely due to the differences in age and BMI, as we have recently shown that clone size may be increased in obese individuals [16].

Our observation that something other than age drives CH prevalence in PWH was substantiated by the fact that the mutational processes underlying the identified CH mutations may be different between PWH and controls. Only in PWH, a ROS mutational signature could be assigned to some of the observed CH mutations. ROS production is indeed increased in PWH and, interestingly, has been linked to nucleoside reverse transcriptase inhibitor (NRTI)-induced mitochondrial toxicity [3, 4]. The enhanced ROS signature found in CH mutations from PWH compared to HIV-uninfected overweight controls could therefore mirror increased mitochondrial dysfunction in PWH. We could not assess whether either HIV or cART use relates to CH mutation development, as all PWH were on cART and with plasma HIV RNA levels <200 copies/mL. However, our data indicate that the ROS signature may contribute to mutations in PWH with prior exposure to zidovudine, whereas it was absent in unexposed individuals. Zidovudine, an NRTI, has been extensively linked to hematological toxicity [28].

The fact that our data suggest that in PWH other processes significantly reduce the correlation of CH prevalence with age is intriguing. Associations between CH and cART duration as well as with age and coronary artery disease were recently reported [11]. However, no correlations with other HIV-related parameters, such as CD4 T-cell count, HIV medication, and HIV reservoir parameters, were reported. We identified that various other HIV-related parameters correlated with CH independent of age, such as CD4 nadir and CD4/CD8 T-cell ratio. CD4 nadir is a marker for the severity of prior

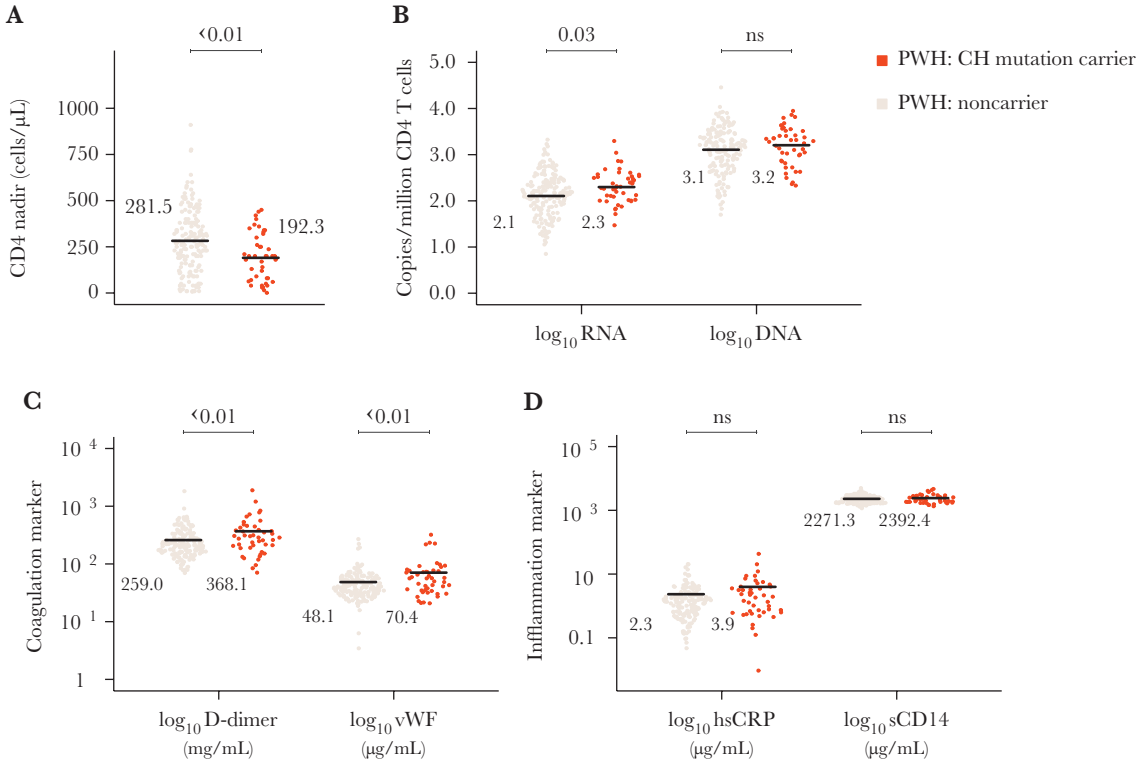

Figure 3. People with HIV (PWH) clonal hematopoiesis (CH) mutation carriers present with significantly lower CD4 nadir, and higher cell-associated HIV RNA and coagulation markers. *A*, Carriers (n = 46) presented with significantly lower CD4 nadir as compared to noncarriers (n = 171). *B*, Carriers (n = 45) showed significantly increased RNA levels as compared to noncarriers (n = 169), and nonsignificantly (ns) increased DNA levels as compared to noncarriers (n = 167). *C*, Carriers (n = 46) presented with significantly increased coagulation markers D-dimer and von Willebrand factor (vWF) as compared to noncarriers (n = 171). *D*, Carriers (n = 45) showed comparable high-sensitivity C-reactive protein (hsCRP) as compared to noncarriers (n = 167) and carriers (n = 46) showed comparable soluble CD14 (sCD14) levels as compared to noncarriers (n = 170). In each plot the mean of noncarriers and CH mutation carriers is annotated with a horizontal bar and value; at the top the Wilcoxon-rank sum test *P* value is given.

immunosuppression and HIV infection course. The link with CD4 nadir suggests prior immunosuppression due to HIV infection is associated with an increased CH prevalence in PWH. Studies have also linked CH to chronic infection and infection risk [28, 29]. Longitudinal studies are needed to further investigate the link between HIV infection and CH. While in HIV-uninfected controls a link between CH and inflammation has been shown [3, 30], no association was found between CH and general inflammation parameters in our cohort of PWH. Our sample size restricted our ability to dissect whether inflammation independent of CD4 nadir has an effect. In contrast, new factors such as HIV reservoir and markers of coagulation—D-dimer and vWF—were independently associated with CH. Besides inflammatory markers, these coagulation factors have also been linked to mortality and CVD and are increased in PWH [27, 31]. The interplay between coagulation, inflammation, and CH requires future mechanistic studies.

The link with HIV reservoir is interesting, considering that several of the most important CH driver genes encode for epigenetic modifiers—genes that modify the epigenome through, for example, DNA methylation—with suggested downstream effects of altered gene expression and increased inflammation [30]. HIV transcription is known to rely on epigenetic modification, cell differentiation, and activation but also low-grade inflammation [1]. It is intriguing to speculate that increased relative HIV-1 transcription in individuals with CH could be the result of an aberrant epigenetic profile, causing alterations in the transcriptional program and cell differentiation [15]. Future studies using single-cell transcriptome analyses in a longitudinal setting could provide mechanistical insight into CH and HIV reservoir dynamics on the single-cell level. These studies could elucidate new mechanisms for (deep) HIV latency and influence future shock and kill strategies in HIV cure [32].

Limitations of the current study include the chosen control populations. The 300-Obese control individuals were processed with the exact same assay and in parallel with PWH, preventing possible confounding due to assay or batch differences, but they were generally older and showed an increased BMI. Although, at the same time, the inclusion of these controls with additional cardiovascular risk factors and older age could underestimate the effect of HIV infection itself on CH, because both age and obesity have been found to be associated with increased prevalence of CH [16]. The comparisons between PWH individuals and population controls are more appropriate due to age- and

sex-matching, but the assay was slightly different and as such we could only validate findings for non-*DNMT3A* mutations. Additionally, our limited sample size restricted the ability to link CH to non-AIDS–related comorbidities, further examine signature analyses, or perform sex-specific analyses. Furthermore, although the reported associations are interesting, the data do not allow us to draw causal inferences. The purpose of this study was exploratory and as such the reported independent correlations should be interpreted as hypothesis generating and require confirmation in future, ideally longitudinally designed, studies. And, finally, our targeted sequencing technique limits unbiased genome-wide CH mutation assessment [3], due to only targeting previously described CH mutation hotspots and genes. Although, this is outweighed by the advantages of this technique—the use of high-sensitivity targeted sequencing including molecular barcoding allows for technical replication, comparable sensitivity, reliable quantification, and overlapping probes ruling out sequencing errors or artefacts [15].

In conclusion, CH in PWH using long-term cART is associated with low CD4 nadir, increased CD4/CD8 T-cell ratio, altered coagulation, and signs of increased HIV transcriptional activity. Future studies on the effect of CH on the HIV reservoir, and non-AIDS–related comorbidities are warranted.

Supplementary Data

Supplementary materials are available at *The Journal of Infectious Diseases* online. Consisting of data provided by the authors to benefit the reader, the posted materials are not copyedited and are the sole responsibility of the authors, so questions or comments should be addressed to the corresponding author.

Notes

Acknowledgments. We thank participants of the Human Functional Genomics Project. We thank the Radboud Genomics Technology Center for technical assistance.

Author contributions. W. H., R. D., A. V. and A. H. designed the study and wrote the manuscript. W. H., L. W., and I. M. recruited and included the participants. W. H. and M. S. performed the laboratory experiments. R. D., M. S., and A. H. generated and analyzed the sequencing data. W. H., R. D., and R. V. analyzed the data and interpreted the data with A. H. and A. V. All authors read and contributed significantly to the final manuscript.

Disclaimer. The financial supporters were not involved in the study design, data interpretation, or the submission.

Financial support. This work was supported by the AIDS Fonds Netherlands; ViiV Healthcare; the Netherlands Organization for Scientific Research (Spinoza grant to M. G. N.); the European Research Council (grant number 833247 Advanced Grant to M. G. N.); and the European Union Horizon 2020 Research and Innovation Program Solve-RD project (grant number 779257 to A. H.).

Potential conflicts of interest. All authors: No reported conflicts of interest. All authors have submitted the ICMJE Form for Disclosure of Potential Conflicts of Interest. Conflicts that the editors consider relevant to the content of the manuscript have been disclosed.

References

1. Borges ÁH, Neuhaus J, Sharma S, et al; INSIGHT SMART; START Study Groups. The effect of interrupted/deferred antiretroviral therapy on disease risk: a SMART and START combined analysis. J Infect Dis **2019**; 219:254–63.
2. Marcus JL, Leyden WA, Alexeeff SE, et al. Comparison of overall and comorbidity-free life expectancy between insured adults with and without HIV infection, 2000–2016. JAMA Netw Open **2020**; 3:e207954.
3. Fuster JJ, Walsh K. Somatic mutations and clonal hematopoiesis: unexpected potential new drivers of age-related cardiovascular disease. Circ Res **2018**; 122:523–32.
4. Bolton KL, Ptashkin RN, Gao T, et al. Cancer therapy shapes the fitness landscape of clonal hematopoiesis. Nat Genet **2020**; 52:1219–26.
5. Jaiswal S, Fontanillas P, Flannick J, et al. Age-related clonal hematopoiesis associated with adverse outcomes. N Engl J Med **2014**; 371:2488–98.
6. Hormaechea-Agulla D, Matatall KA, Le DT, et al. Chronic infection drives Dnmt3a-loss-of-function clonal hematopoiesis via IFNγ signaling. Cell Stem Cell **2021**; 28:1428–42.e6.
7. Jaiswal S, Libby P. Clonal haematopoiesis: connecting ageing and inflammation in cardiovascular disease. Nat Rev Cardiol **2020**; 17:137–44.
8. Jaiswal S, Libby P. Author correction: clonal haematopoiesis: connecting ageing and inflammation in cardiovascular disease. Nat Rev Cardiol **2020**; 17:828.
9. Appay V, Almeida JR, Sauce D, Autran B, Papagno L. Accelerated immune senescence and HIV-1 infection. Exp Gerontol **2007**; 42:432–7.
10. Hunt PW, Lee SA, Siedner MJ. Immunologic biomarkers, morbidity, and mortality in treated HIV infection. J Infect Dis **2016**; 214 (Suppl 2):S44–50.
11. Bick AG, Popadin K, Thorball CW, et al. Increased CHIP prevalence amongst people living with HIV. medRxiv, doi: 10.1101/2020.11.06.20225607, **7** November **2020**, preprint: not peer reviewed.
12. Watson CJ, Papula AL, Poon GYP, et al. The evolutionary dynamics and fitness landscape of clonal hematopoiesis. Science **2020**; 367:1449–54.
13. Van der Heijden WA, Van de Wijer L, Keramati F, et al. Chronic HIV infection induces transcriptional and functional reprogramming of innate immune cells. JCI Insight **2021**; 6:e145928.

14. Ter Horst R, van den Munckhof ICL, Schraa K, et al. Sex-specific regulation of inflammation and metabolic syndrome in obesity. Arterioscler Thromb Vasc Biol **2020**; 40:1787–800.
15. Acuna-Hidalgo R, Sengul H, Steehouwer M, et al. Ultra-sensitive sequencing identifies high prevalence of clonal hematopoiesis-associated mutations throughout adult life. Am J Hum Genet **2017**; 101:50–64.
16. van Deuren RC, Andersson-Assarsson JC, Kristensson FM, et al. Expansion of mutation-driven haematopoietic clones is associated with insulin resistance and low HDL-cholesterol in individuals with obesity. bioRxiv, doi: 10.1101/2021.05.12.443095, **9** July **2021**, preprint: not peer reviewed.
17. Li H, Durbin R. Fast and accurate short read alignment with Burrows-Wheeler transform. Bioinformatics **2009**; 25:1754–60.
18. Weren RD, Mensenkamp AR, Simons M, et al. Novel *BRCA1* and *BRCA2* tumor test as basis for treatment decisions and referral for genetic counselling of patients with ovarian carcinomas. Hum Mutat **2017**; 38:226–35.
19. Eijkelenboom A, Kamping EJ, Kastner-van Raaij AW, et al. Reliable next-generation sequencing of formalin-fixed, paraffin-embedded tissue using single molecule tags. J Mol Diagn **2016**; 18:851–63.
20. Li H, Handsaker B, Wysoker A, et al; 1000 Genome Project Data Processing Subgroup. The sequence alignment/map format and SAMtools. Bioinformatics **2009**; 25:2078–9.
21. Jaiswal S. Clonal hematopoiesis and nonhematologic disorders. Blood **2020**; 136:1606–14.
22. van der Vorm LN, Li L, Huskens D, et al. Analytical characterization and reference interval of an enzyme-linked immunosorbent assay for active von Willebrand factor. PLoS One **2019**; 14:e0211961.
23. Rutsaert S, De Spiegelaere W, De Clercq L, Vandekerckhove L. Evaluation of HIV-1 reservoir levels as possible markers for virological failure during boosted darunavir monotherapy. J Antimicrob Chemother **2019**; 74:3030–4.
24. Trypsteen W, Vynck M, De Neve J, et al. ddpcRquant: threshold determination for single channel droplet digital PCR experiments. Anal Bioanal Chem **2015**; 407:5827–34.
25. Alexandrov LB, Kim J, Haradhvala NJ, et al; PCAWG Mutational Signatures Working Group; PCAWG Consortium. The repertoire of mutational signatures in human cancer. Nature **2020**; 578:94–101.
26. Rosenthal R, McGranahan N, Herrero J, Taylor BS, Swanton C. DeconstructSigs: delineating mutational processes in single tumors distinguishes DNA repair deficiencies and patterns of carcinoma evolution. Genome Biol **2016**; 17:31.
27. Pasternak AO, Berkhout B. What do we measure when we measure cell-associated HIV RNA. Retrovirology **2018**; 15:13.
28. Richman DD, Fischl MA, Grieco MH, et al. The toxicity of azidothymidine (AZT) in the treatment of patients with AIDS and AIDS-related complex. A double-blind, placebo-controlled trial. N Engl J Med **1987**; 317:192–7.
29. Zekavat SM, Lin SH, Bick AG, et al; Biobank Japan Project; FinnGen Consortium. Hematopoietic mosaic chromosomal alterations increase the risk for diverse types of infection. Nat Med **2021**; 27:1012–24.
30. Challen GA, Goodell MA. Clonal hematopoiesis: mechanisms driving dominance of stem cell clones. Blood **2020**; 136:1590–8.
31. Gutekunst KA, Kashanchi F, Brady JN, Bednarik DP. Transcription of the HIV-1 LTR is regulated by the density of DNA CpG methylation. J Acquir Immune Defic Syndr **1993**; 6:541–9.
32. Cohn LB, Chomont N, Deeks SG. The biology of the HIV-1 latent reservoir and implications for cure strategies. Cell Host Microbe **2020**; 27:519–30.